Received 17 April 2018; revised 9 June 2018; accepted 27 June 2018. Date of publication 3 July 2018;
date of current version 24 July 2018. The review of this paper was arranged by Editor S. Vaziri.

Digital Object Identifier 10.1109/JEDS.2018.2852288

Inkjet Printed Electrodes in Thin Film Transistors

RUIQIANG TAO[1], HONGLONG NING[1], JIANQIU CHEN[1], JIANHUA ZOU[1], ZHIQIANG FANG[2], CAIGUI YANG[1], YICONG ZHOU[1], JIANHUA ZHANG[3], RIHUI YAO[1], AND JUNBIAO PENG[1]

1 State Key Laboratory of Luminescent Materials and Devices, Institute of Polymer Optoelectronic Materials and Devices, South China University of Technology, Guangzhou 510640, China
2 State Key Laboratory of Pulp and Paper Engineering, South China University of Technology, Guangzhou 510640, China
3 Key Laboratory of Advanced Display and System Applications of Ministry of Education, Shanghai University, Shanghai 200072, China

CORRESPONDING AUTHORS: H. NING AND R. YAO (e-mail: ninghl@scut.edu.cn; yaorihui@scut.edu.cn)

This work was supported in part by the National Key Research and Development Program of China under Grant 2016YFB0401504, in part by the National Natural Science Foundation of China under Grant 51771074, Grant 51521002, and Grant U1601651, in part by the National Key Basic Research and Development Program of China (973 Program) Founded by MOST under Grant 2015CB655004, in part by the National Science Foundation for Distinguished Young Scholars of China under Grant 51725505, in part by the Guangdong Natural Science Foundation under Grant 2016A030313459 and Grant 2017A030310028, in part by the Guangdong Science and Technology Project under Grant 2016B090907001, Grant 2016A040403037, Grant 2016B090906002, Grant 2017B090907016 and Grant 2017A050503002, and in part by the Guangzhou Science and Technology Project under Grant 201804020033.

ABSTRACT Inkjet printing is a non-vacuum, non-contact, low-cost, and direct patterning thin film deposition technique. Compared to traditional processes, it demands less materials and energy, simplifies processing steps and is compatible with the fast fabrication of flexible and large-size devices, thus potential in the application of thin film transistors. In this paper, we have compared the main techniques of inkjet printing, and discussed the formulation of conductive inks, the deposition of high quality electrodes, and the obtaining of high resolution and high performance thin film transistors. Moreover, the faced problems and corresponding solving methods of inkjet printed thin film transistor with low sintering temperature, small line width, short channel, high mobility, and designed structure are summarized by the understanding of the interaction among inkjet printing devices, materials, processes, and the fabrication of transistors, which providing referential significance of the following research effort.

INDEX TERMS Inkjet printing, thin film transistors, electrodes, low-temperature techniques, high performance.

I. INTRODUCTION

The fabrication of thin film transistors (TFT) using full vacuum process requires expensive devices, advanced materials, and time costs. Compared with traditional vacuum deposition technology, inkjet printing has the following advantages in the preparation of TFT electrodes films: 1) Non-vacuum environment, which saves energy and simplifies film forming process; 2) Saving materials in a drop on demand (DOD) way; 3) Direct pattering of functional layers. Although the graphic precision is not as good as the traditional process such as lithography, it avoids the electrical damage of other functional layers caused by the process of developing, and is more compatible with flexible substrate [1]; 4) Contactless deposition process, which avoids pollution and mechanical damage; 5) High throughput and potential in the fabrication of large size and large scale electronics [2]–[10].

TFT electrodes, which is applied in high cost-effective display devices, is usually required to have the characteristics of high conductivity, low cost, thermal resistance, oxidation resistance, etc. Moreover, ink chemistry, film forming, surface modification, and post treatment remained challenges in inkjet printing: 1) Conductive ink need to meet both the printing conditions and the electrical requirements devices; 2) Inkjet printing process includes droplets jetting, fighting, impinging and evaporation after deposition [11], [12], thus it is affected by printers, ink characteristics, jetting conditions, substrate states, drying processes, etc. 3) Surface modification and post treatment are related to the electrodes morphology, solute distribution, additive residue and electrical performance. Conductive inks for inkjet printing often has problems such as low resolution, satellite point, coffee ring, high resistivity, and poor electrodes/semiconductor contact characteristics. Various factors such as equipment, materials, and processes need to be comprehensively considered in the solutions.

The integration of inkjet printed electrodes and TFT devices faces new problems: 1) Low temperature sintering of conductive materials, which is compatible with flexible

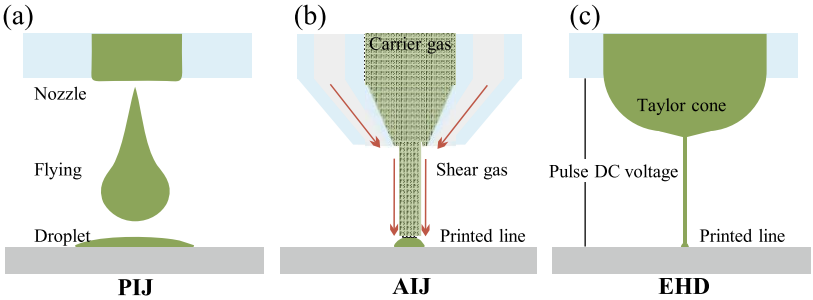

FIGURE 1. Types of inkjet printing. (a) Conventional piezoelectric inkjet printing. (b) Aerosol Jet gel printing. (c) Electro-hydrodynamic printing.

substrate, and at the same time to achieve its low resistivity; 2) Small line width, short channel, high uniformity, and high adhesion electrodes deposition technologies; 3) High mobility, low signal delay, and low leakage current TFT devices. Inkjet printed TFT electrodes is required to solve the problems above, while taking into account of the ink printability, electrical damage to functional layers, and elements diffusion. Moreover, considering the interrelated factors such as device structure, material selection, thin film deposition, post treatment, interface and surface characteristics is crucial to realize high performance and high resolution TFT devices.

II. INKJET PRINTING AND CONDUCTIVE FILMS

A. INKJET PRINTER

There are many kinds of inkjet printers, but the most popular three technologies in electronics manufacturing are Piezoelectric inkjet printing (PIJ), Electro-hydrodynamic printing (EHD), and Aerosol inkjet printing (AIJ) (Fig. 1).

There are significant differences in the driving mode of theses printers. Piezoelectric ceramics deforms in the conventional PIJ by applying periodic waveform voltage to drive the injection of tiny droplets. High voltage (kilovolt level) is applied between the nozzle and the substrate in EHD to form a Taylor cone, while low-frequency pulse voltage signal is used to drive the ink to spray out in droplets, and the high-frequency pulse DC voltage signal drives the ink to be ejected continuously and linearly. It breaks the nozzle size limit in high precision printing, but the whole injection process is affected by the electricity of materials and substrate, which is unfavorable to the fabrication of electrical devices. By dispersing ink in air carrier to form aerogel, AIJ sprays linear fluid continuously under the controlling of the shearing air beam, and uses ink receiver to achieve droplets printing. It has a certain application prospect, due to its high resolution patterning capability without requirement of electrical properties of materials. The selection of the specific printing method needs to be considered comprehensively according to the practical application. Table 1 compares the three ways [13]–[15].

EHD is especially suitable for high precision printing, but the limitation of materials electricity make it mostly used in the preparation of conductive layer. AIJ is not restricted by rigidity, electricity and surface smoothness of substrate.

TABLE 1. Comparison of advantages and disadvantages of three mainstream inkjet printing techniques.

Printing techniques	Advantages	Disadvantages
PIJ	1) No Electrical requirements for materials; 2) Cost-effective; 3) High integration; 4) Flexible fabrication; 5) Stable.	1) Line width > 20 μm; 2) Viscosity <30 cps; 3) Nozzle block.
EHD	1) Sub-femtolitrer droplets; 2) Line width of 1 μm; 2) Viscosity < 50000 cps; 3) 3D patterns.	1) Electrical requirements for materials; 2) Low viscosity for dots and dielectric materials; 3) Electro-wetting.
AIJ	1) Line width < 10 μm; 2) Viscosity < 2000 cps; 3) No Electrical requirements for materials; 4) Flexible fabrication; 5) 3D patterns; 6) Nozzle not easily blocked.	1) Satellite points; 2) Complex system; 3) Low integration; 4) Expensive.

Immediate drying deposition process make it suitable for high aspect ratio narrow wire printing [16]. Without solvent damage to bottom layers, AIJ is especially compatible with multi-layer devices, like TFTs, *et al.* [17], [18]. PIJ is stable, but will cause problems such as droplets spreading and the coffee ring effect due to the strong effect of the solvent, which affects the graphic accuracy and uniformity. However, there's no requirement for electrical properties of materials, which is suitable for functional layers printing, and is the most likely to be used in industrialization.

There are two trends in new developed inkjet printing techniques: 1) To improve the precision in motion and alignment, and integrate multiple print heads with various printing technologies to completely meet the high resolution, high performance and high throughput requirements of electronics fabrication [19], [20]. However, the system is complex and expensive. 2) To explore novel printing mechanism. For example, using a super-fine inkjet printing (SIJ), 1 μm line width and 2.5 μm line spacing can be achieved [21]. EHD and SIJ both use oscillatory electric field to generate droplets, but the jetting of fluid by SIJ is no longer dependent on the formation of the Taylor cone. The driving voltage is smaller, and the conductivity

TABLE 2. Previous work on thin film transistor with aerosol inkjet printed electrodes.

Electrodes	Semiconductor	Mobility ($cm^2V^{-1}s^{-1}$)	Log(On/off ratio)	Reference	Year
Au	P3HT	1.8	5	[23]	2008
Au	P(NDI2OD-T2)	0.85	6	[24]	2009
PEDOT：PSS Graphene	Graphene	1188±136（hole） 422±52（electron）	<1	[25]	2011
PEDOT：PSS	P3HT	1	5	[26]	2012
Ag	SCNT	1	3	[27]	2012
Ag	SCNT	1.5	3	[28]	2012
PEDOT:PSS	P3HT	1.3	6	[29]	2013
Graphene oxide	Graphene oxide	350	<1	[18]	2013
PEDOT:PSS	SCNT	32.3	6	[30]	2014
Ag	SCNT	34.8	5	[31]	2014
Al	IGZO	0.75	4	[32]	2015
Ag	SCNT	16.1	4	[33]	2017

requirement of the ink and the substrate (even the insulating substrate) is lower. However, tiny nozzle used is easy to block. Moreover, micron scale nozzle-substrate distance is not compatible with flexible preparation. The printing process is still highly dependent on the driving electric field, and can be influenced by charge accumulation (long time printing) and environmental factors (such as humidity), which may lead to unstable jetting of droplets [22]. Compared to these two techniques, AIJ is more appropriate for electronics fabrication, and the solvent damage can be avoided to other functional layers. Table 2 summaries the TFT characteristics with AIJ printed electrodes [18], [23]–[33]. However, the high cost and low integration limits its use in industrialization. Up to now, there is no inkjet printing equipment with excellent performance in all aspects. The integration of various inkjet printing technologies is potential in the fabrication of printed electronics.

B. CONDUCTIVE INKS

Conductive ink has challenge in its formulation, which determines the printability, equipment maintenance, metallization process and electrodes performance. Especially in the fabrication of flexible TFTs, jetting stability, uniform deposits, low sintering temperature (<150 °C), high conductivity, and good contact characteristics of the electrodes/semiconductor interface are all required.

Ink printability is a prerequisite for its preparation. Taking PIJ for example, the Ohnesorge number (Oh) can be used to approximately determine droplets jetting behavior [34], [35]. It removes the fluid jetting velocity criterion, thus has more reference value for ink preparation before printing. Droplet jetting inertia, surface tension and viscoelasticity determines the value of Oh, which can be expressed by

$$Oh = \frac{\sqrt{We}}{Re} = \frac{\eta}{\sqrt{\rho\gamma L}} \tag{1}$$

Where ρ is fluid density, L is the diameter of droplet, γ is surface tension, η is viscosity. The suitable range of printing is $0.1 < Oh < 1$. If Oh is too large, the viscous dissipation prevents the droplet from deforming and make it difficult to spray out. If Oh is too small, satellite points appear under the balance of surface tension and viscosity. This method does not take into account that the satellite points are incorporated into the main droplet, when Oh is much less than 0.1. Moreover, the value may be slightly deviated under practical conditions [36]. The L is related to the equipment, ρ and γ are mainly related to the solvent, while η is affected by many factors, such as polymer additive, shear rate, temperature *et al.* Therefore, the ink preparation in inkjet printing is complex.

Solutes of conductive inks usually are conjugated polymers [37], inorganic materials, and other special materials (graphene [38], carbon nanotubes [39], etc.). Common materials and their characteristics are shown in Table 3. Inorganic metal materials can meet the high conductivity interconnection requirements of high performance TFT backplane. High biocompatibility gold nanoparticles inks are often used in the field of bioelectronics. Silver has advantages

TABLE 3. Comparison of advantages and disadvantages of different conductive inks.

Types	Materials	Advantages	Disadvantages
Conjugated polymers	Polyaniline, Polypyrrole, PEDOT, etc.	1) Good printability; 2) Low production cost; 3) Deformable.	1) Low conductivity; 2) Poor electrical stability; 3) Poor thermal stability.
Inorganic materials	ITO, Au, Ag, Cu, Al, etc.	1) High conductivity; (except for ITO); 2) easy access to materials.	Poor solution processability
Special materials	Graphene, CNT, etc.	1) High strength; 2) Low impurity, 3) Good solution processability	Not easy to prepare

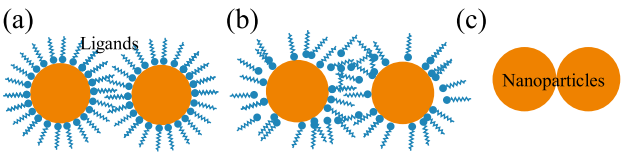

FIGURE 2. States of nanoparticles structure before and after inkjet printing. (a) Ink preservation state; (b) Solvent evaporation and ligand destruction; (c) After sintering.

in cost, conductivity [40], [41], antioxidation property and water dispensability, thus is the most used currently. It has entered commercial production in the United States, Japan, South Korea, Israel and other countries. Although copper, aluminum, etc. are even cheaper, they are easily oxidized in atmospheric environment. They generally require hydrocarbon solvents, low precursor concentrations, and an inert storage and process atmosphere [42]. At present, low resistivity and low temperature sintering of copper ink can be achieved by using a strong pulsed laser, but the research of TFT devices with printed copper electrodes remains a big challenge [43]. Conductive ink can be divided into nanoparticles inks and precursor inks.

B.1. NANOPARTICLES INKS

Nanoparticles are coated with polymeric ligand materials to achieve stable dispersion in the solvent [44]. The basic structure is shown in Fig. 2a. In different stages of the printed electrodes film formation process, the nanoparticles structure changes significantly (Fig. 2b and Fig. 2c).

Ligand materials usually use long alkyl chains with polar heads, such as thiols, carboxylic acids [45], and amine polymers to prevent nanoparticles agglomeration through steric stabilization, bridging, or flocculation mechanisms. Solvent selection must take into account of physical properties such as density, boiling point, viscosity, and surface tension. Besides, processability, solute solubility, and thermal stability should also be considered. Usually toluene, xylene, ethanol, diethyl titanate, methyl ethyl ketones, tetradecanes and other near-linear polymer organic solvents are used in ink system, but considering environmental factors it also have water as solvent [46]. Solvent types determine the basic properties of the ink (viscosity, surface tension, wettability) and affects the print quality of the film (droplet size, positioning accuracy, satellite points formation, and substrate wetting).

TABLE 4. Common materials and uses of nanoparticle ink additives.

Ink additives	Common materials	Uses or mechanisms
Viscosity modifier	Non-adsorptive polymers: high molecular weight polyethylene glycols, etc.	Make ink viscosity continuously adjustable
Adhesive	Usually resin	Increase film adhesion after sintering
Moisturizer	Urea, glycerol, etc.	Strong hydrogen bonding networks prevents unwanted solvent evaporation
Humectant	Glycol ethers, etc.	Adjust the wetting behavior of droplets on substrate
Buffer	Ionic polyacrylates, etc.	Prevents the pH of the dispersion from gradually decreasing over time (the adsorption of CO_2)

Nanoparticles dispersion system requires the addition of different additives to achieve high performance and high stability in the printing process [47]. The common materials of different additives and their uses are shown in Table 4. The mutual influence of each additive often makes the actual ink configuration process more complicated. High concentration of moisturizer can adjust the viscosity. Wetting agent has surface activity, and its high concentration will affect the printability and film quality. Some phosphatidic acid or organic buffer contains a large proportion of electrolyte, which will affect the stability of the dispersion. In addition, solvent viscosity, ink concentration, solutes size and shape, and various additives can affect the rheological properties of the ink, which in turn affects the jetting behavior of the ink [48], [49]. Commercialized nanoparticles conductive inks, which have advantages in low cost, high performance, long life, and printable features, are still rare.

B.2. PRECURSOR INKS

Precursor ink is usually a metal-organic decomposition ink, which uses the decomposition of organic components and salts to generate metal components [50], [51], or an ink system with the addition of reducing agents to metal salt solution [52]. Both of the inks can be converted into conductive metal wires by heat treatment or the like, and are easily realized by a low sintering temperature. Printing film using precursor ink has excellent uniformity and performance, but it is inferior to the durability of the nanoparticles ink (water resistance and light resistance). Table 5 shows the advantages and disadvantages of the two inks [53]–[55].

TABLE 5. Comparison of advantages and disadvantages of three mainstream inkjet printing techniques.

Ink types	Advantages	Disadvantages
Nanoparticles (suspension)	1) Good chemical stability; 2) Good weather resistance (water, light, etc.); 3) Higher solid content; 4) Adjustable ink system for high film adhesion..	1) Particles are easy to agglomerate; 2) High-concentration, large-particles are easy to plug the nozzle; 3) The surface of the film is poor in flatness; 4) Increase in solid content will affect the viscosity and droplet ejection.
Precursor (sulution)	1) Without solutes agglomeration; 2) Nozzles are not easy to block; 3) Easy to configure, including water-soluble ink; 4) Smooth surface of the film; 5) Friction resistance; 6) High conductivity.	1) Poor chemical stability; 2) Poor weather resistance (water, light, etc.); 3) Higher contact resistance.

C. LOW-TEMPERATURE PROCESSING

Metal inks need to achieve conductivity close to the bulk material to reduce parasitic electrode voltage drop [1]. On a flexible substrate, thermal deformation will influence the high-resolution patterning and the precise alignment between different layers of the device. Considering the high coefficient of thermal expansion of the plastic film, the maximum process temperature should be lower than the glass transition temperature of the substrate, which is generally lower than 150 °C, and the best is about 100 °C.

For metal nanoparticles inks, metal core surface coverage ligand molecules are generally insulating materials. Ligand residues will affect the electrical conductivity, so that the conductivity of printed metal wire smaller than the pure metal. While changing the metal work function, the formation of energy barriers will affect the electrical performance of printed electrode's TFT device [56]. At present, there are various low-temperature sintering methods that are compatible with the preparation of flexible electronic devices: 1) Low-temperature thermal sintering; 2) Novel sintering methods such as electricity [57], infrared light [58], ultraviolet light [59], [60], flash [61], laser [62]–[65], microwave [66], plasma [6] and other low-temperature sintering of the film. Among them, thermal sintering is still the most commonly used sintering method because of its low equipment cost, simple process, and broad prospects for industrialization.

Reducing the thermal sintering temperature mainly proceeds from the following three points: 1) Low resistance targets with conductive ligands [67]; 2) Change in particle shape. Studies have shown that silver nanowire inks have a relatively lower sintering temperature than silver nanoparticles (spherical) [2], [68]; 3) The metal precursor ink is easy to obtain high performance through low temperature sintering, although its life is too short, and the weather resistance of the film is poor. Table 6 summarizes high-performance low temperature sintering silver inks, where the 300 °C sintering process ink is used as a comparison [69]–[79].

The reduction of nanoparticles size is one of the keys to low-temperature sintering of high-melting-point metal inks. The reasons are as follows: 1) Quantum size effects; 2) Large specific surface area of nanoparticles [80]. Surface atoms occupy a higher proportion, while surface atoms have fewer adjacent atoms and fewer metal bonds, relative to bulk materials. The atomic binding energy is small, which leads to a lower melting point [45], [81]. For example, the bulk gold metal has a melting point of 1063 °C, but the 2.5 nm diameter gold nanoparticles has a melting point of 500 °C [80], and the 1.5 nm diameter gold nanoparticles has a even lower melting point of 380 °C [81]. 3) The melting point of the conductive ink is not equal to the sintering process temperature. Small size particles have a lower melting point and higher atomic diffusion rates. Under low temperature conditions, interparticle fusion is enhanced by diffusion of its interfacial atoms. Therefore, under the condition of small particle size, the destruction temperature of the ligand actually determines the process temperature for forming the conductive channel between the metal particles. When the particles lose the organic shell, direct contact between particles starts to show electrical conductivity. Further temperature rise promotes the growth of the particle fusion region, which reduces the resistivity and the make the film denser [45].

Low temperature sintering processes for metal inks are also currently rapidly developing, and some of the new sintering methods have great potential in the preparation of flexible electronic devices, such as chemical sintering, vapor reduction sintering, hot water assisted sintering, and photo reduction sintering [82]. Chemical sintering changes the printed pattern from non-conductive to conductive by adding chemical components to the printed ink. Based on different sintering mechanisms for different types of ink systems, the method can be subdivided into electrolyte sintering [83]–[88], reducing agent sintering [89], microreactor in-situ synthesis [90] (Fig. 3a), reactive inkjet printing systems [91] (Fig. 3b), and the like. During the sintering process, the decomposition of the stabilizer will form pores, which will reduce the conductivity of the silver film. Moreover, there are some methods for metal-organic precursor inks. Wu *et al.* [92] placed $AgNO_3$/PVP print patterns in ethylene glycol vapor at 250 °C for reduction and sintering for 10 min, finally obtaining a conductive silver wire resistivity of 27.1 μΩ·cm (Fig. 3c). Koga *et al.* [93] spin-coated presursor ink onto a PEN substrate and used a dryer to pre-dry it at 80 °C to obtain a silver nanoparticles film with a resistivity of 1.9×10^3 μΩ·cm. It was then immersed in hot water at 80 °C for 5 minutes, and the resulting film was dried at room temperature to reduce its resistivity to 5.9 μΩ·cm (Fig. 3d).

TABLE 6. High performance and low temperature processed inks.

Source	Complexation/ Dispersion	Reducing	Sintering (°C)	Resistivity (μΩ·cm)	Reference
$AgNO_3$	-	-	300	15	[58]
$AgNO_3$	Saturated decanoate	$N_2H_4{\cdot}H_2O$	300	6.1	[59]
$AgNO_3$	PVP	Ethylene glycol	200	10	[60]
$AgNO_3$	Lauric acid	$N_2H_4{\cdot}H_2O$	200	8.1	[61]
$AgNO_3$	Lauric acid	$NaBH_4$	125	6.6	[62]
$AgNO_3$	1-Dimethylamino-2-propanol	1-Dimethylamino-2-propanol	100	17.3	[63]
CH_3COOAg	Ethylamine+ ethanolamines	HCOOH	150	4.1	[64]
CH_3COOAg	Ammonia+ ethylamine	HCOOH	90	19.8	[65]
CH_3COOAg	Ammonia	HCOOH	90	1.6	[66]
Silver citrate	1,2-diaminopropane	-	150	17.8	[67]
Silver oxalate	Ethylamine	-	150	8.4	[68]

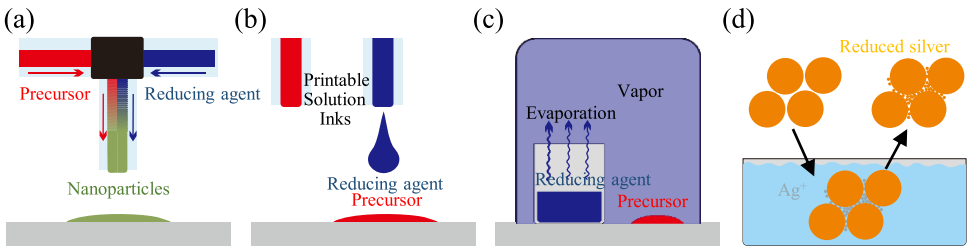

FIGURE 3. Low temperature sintering techniques. (a) Microreactor in-situ synthesis; (b) reactive inkjet printing systems; (c) Vapor reduction sintering; (d) Hot water assisted sintering.

III. INKJET PRINTED ELECTRODES IN TFTS

Printed electronics are generally used in low-end applications and have the advantages of low cost, mass production, and flexibility, but exploration for the preparation of high performance electronic devices is undergoing. Inkjet printing TFT mobility [94], pattern resolution, pattern accuracy (pattern repeatability) and large size uniformity are the main influencing factors to achieve high resolution, large size display. For a single TFT device, the focus is on high resolution electrodes patterning and its increased mobility.

A. HIGH-RESOLUTION ELECTRODES INKJET PRINTING

High resolution electrodes inkjet printing relies on equipment upgrades and surface treatments. In general, the resolution of inkjet printed graphics can be given by the printed line width and spacing. Although the equipment largely determines the final resolution of the image, here only the traditional piezoelectric inkjet printing technology is taken as an example to explore possible problems encountered in obtaining small line width, short channel, high uniformity, high adhesion electrode films.

A.1. SMALL LINE WIDTH

Line width of inkjet printing is constrained by many factors: 1) The high conductivity requirement of the printed line: From the perspective of inkjet printing, the final conductivity can be achieved by increasing the number of printing layers and reducing the distance between ink droplets. Teng and Vest [51] found that the square resistance of silver wire inkjet printed for four to five layers can be comparable to that of vapor deposited silver, but increasing the number of printed layers or reducing the distance between ink droplets will increase the line width; 2) The nozzle geometry limits the volume of the ejected droplets, and thus affect the line width: The formation of inkjet printed lines is followed by droplet ejection, flight, impacting the substrate, spreading, and droplets merging. The line's formation model is shown in Fig. 4a. It can be seen that the line width is related to

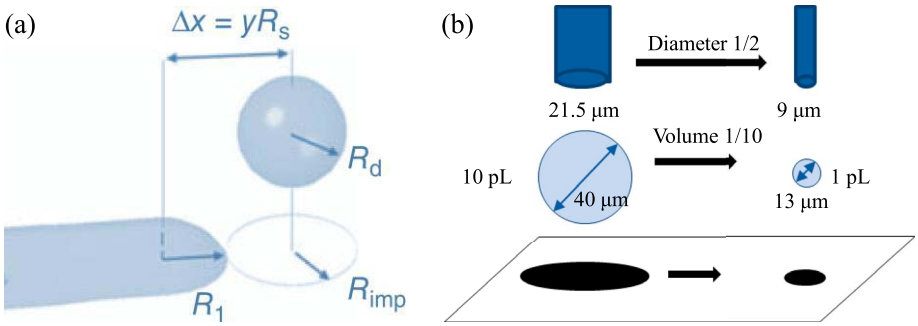

FIGURE 4. (a) Line formation model; (b) Pattern resolution of piezoelectric inkjet printing limited by nozzles.

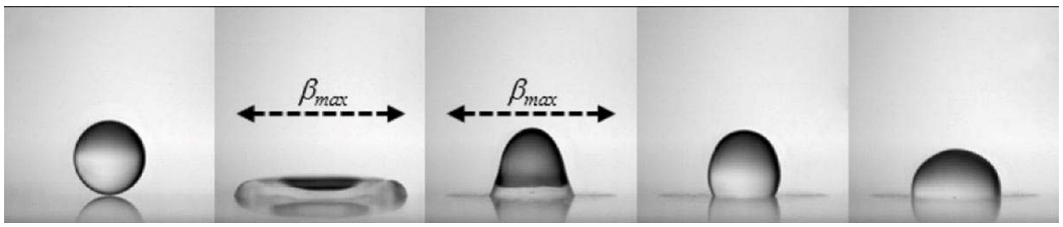

FIGURE 5. Dynamics of a droplet impacting a solid substrate. Copyright 2014 Springer-Verlag Berlin Heidelberg.

the size of the ejected droplets, and its relation is:

$$\frac{d}{2} = R_1 = \sqrt{\frac{8}{3}\left(\frac{R_d^3\psi}{\Delta x}\right)}, \tag{2}$$

$$\psi = \frac{\pi}{2}\left(\frac{\sin^2\theta_s}{\theta_s - \sin\theta_s\cos\theta_s}\right) \tag{3}$$

$$R_{imp} = \Delta x - R_1 \tag{4}$$

d, line width; R_{imp}, diameter of droplet base; R_1, radius after droplet fusion; R_d, radius of flying droplet; Ψ, geometric function related to static contact angle of droplet; Δx, droplet spacing; θ_s, static contact angle of droplet; R_s The maximum spreading radius of the droplet; R_{imp}, the radius of the droplet in contact with the droplet of the preceding droplet.

From Equation (3) it can be seen that the printed line width has the largest correlation with the three parameters of droplet size, droplet spacing, and droplet static contact angle. The maximum droplet spreading radius R_s needs to be considered when ejecting droplets to form a line. The droplet spacing needs to satisfy at least $2R_1 \leq \Delta x < R_1 + R_s$. If the droplet spacing is too small, the printed line forms a bulge, and if the line is too large, the printed line is discontinuous. The contact angle is related to the ink and the surface energy of the substrate. Droplet size is also limited by the printing device and ink properties.

As shown in Fig. 4b, the minimum ejected droplet diameter of PIJ is limited by the nozzle geometry compared to EHD and AIJ. When using a 9-μm-diameter nozzle, the ejected droplet diameter can reach 13 μm (the volume is approximately 1 pL) and the printed line width can reach 20 μm. However, in this case, the ink chemistry and a higher ejection pressure are required. Due to the difficulty in tailing of the ejected fluid, the printed image is often accompanied by many satellite points, which greatly limits the realization of the ideal performance of inkjet printed materials.

A.2. SHORT CHANNEL

At present, many research groups have demonstrated that printed TFTs can achieve high performance [95]–[97], but most high-performance devices require additional intermediate process steps. One of the reasons for this is the short channel formation between source and drain (SD) electrodes [98]. The cutoff frequency (f_T) and the drain current (I_D) expression of the TFT under saturation are shown as follows [99]:

$$f_T \approx \frac{\mu_{eff}(V_{GS} - V_{TH})}{2\pi L(L + 2L_C)} \tag{5}$$

$$I_D = \frac{V_D\mu_0 C_i W(V_{GS} - V_{TH})}{L + \mu_0 C_i W R_C(V_{GS} - V_{TH})} \tag{6}$$

μ_{eff}, effective carrier mobility; L, channel length; L_C, contact length (electrodes offset); V_{GS}, gate-source voltage; V_{TH}, threshold voltage; μ_0, semiconductor intrinsic mobility; C_i, gate dielectric capacitance per unit area; R_C, contact resistance; W, channel width.

The L_C is related to the parasitic capacitance and it can be reduced when the device size is reduced by improving the alignment accuracy. In addition to reducing the L_C, the reduction of the channel length L is an effective way to achieve a high cut-off frequency while ensuring the effective mobility of the same TFT device, enabling the device to run fast and increase its source-drain current I_D at the same time.

Inkjet printed droplets impact the substrate through the following processes: impact, spreading, relaxation, wetting, balancing [100] (Fig. 5). Its maximum spreading radius

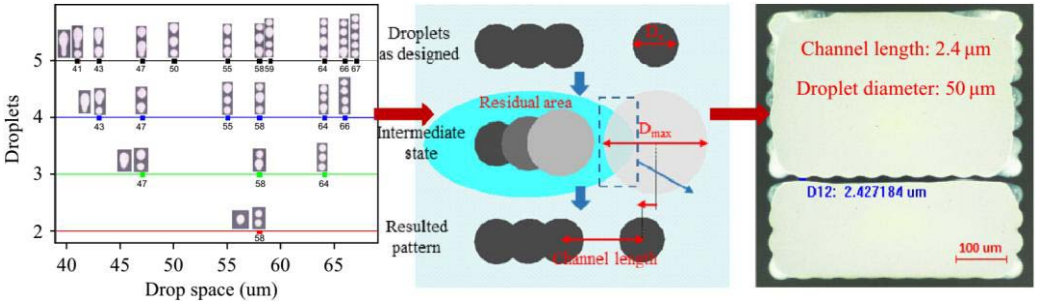

FIGURE 6. **Schematic of short channel direct inkjet printing technology.**

$D_{max} = D_0\beta_{max}$ is shown as follows:

$$\beta_{\max} \sim We^{\frac{1}{4}} \tag{7}$$

$\beta_{\max}$, the maximum spreading factor of droplet; *We*, the Weber number. The maximum spreading radius of droplets is related to ink density and surface tension. The minimum channel length is related to the difference between the droplet's maximum spreading radius and its equilibrium radius, so the shortest channel is affected by the substrate surface energy, temperature, and ink properties. Although the low surface energy of the substrate can prevent droplet spreading, it can destabilize the pattern and cause the printed line to break into individual droplets [101].

The droplet volume of inkjet printing and the droplet spreading are difficult to control, thus the channel length, which can be stably repeated, is often limited to 50-100 μm [98]. To reduce the channel length, researchers have made many attempts with optimized substrate surface energy, temperature, and printing conditions: 1) To reduce the droplet volume by using very fine nozzles (Subfemtoliter level [102]) or using EHD, SIJ, etc. to obtain a channel length of 1-10 μm [103], [104], this method is premised on the sacrifice of printing throughput; 2) Printing a single electrode and then ablate the channel by laser [105]; 3) Photolithography of the substrate to form a bounded droplet spreading [106]; 4) Pre-patterning the substrate wettability (UV treatment [82], [107], light etching or plasma etching of the substrate [108]); 5) Using the coffee ring effect to form adjacent lines [8]; 6) The first drop of ink is treated with a fluoride self-assembling monolayer (SAMs) (deposit CF_4, Plasma, or add surfactant to reduce the surface energy of the first droplet) to repel it from the second drop, self-aligned to form a sub-micron channel at 100 nm scale [109], [110]. With a channel length of 100 nm, a fast switching of the organic TFT frequency of 1.6 MHz can be achieved [95].

The above methods are effective, but they are more complicated, time consuming and increase the cost. Doggart *et al.* printed the second electrode by self-aligning to form a short channel as low as 10 μm by preprinting hydrophobic boundary residue caused by the retraction of the first electrode on the hydrophilic substrate [98]. Although the method is simpler, it still requires surface modification or requirements on the hydrophilicity of the substrate and the material itself. Recently, Ning *et al.* for the first time formed a 2.4 μm ultrashort channel by effectively controlling the growth of electrodes film interspace defects (Fig. 6) [111]. This method does not require any additional process, is simple and repeatable, and provides a reference for direct patterning of short channel by inkjet printing.

In the short channel device array preparation process, some devices are prone to short circuit and the yield is low. The traditional electrodes pattern generally adopts a parallel design in inkjet printing. Splashing or spreading of droplets in some areas may cause a short circuit between the SD electrodes. Caironi *et al.* used a method of forming a short channel by self-aligned printing with SAM layer (Fig. 7), and achieved a 94-100% high yield of short channel (200 nm-400 nm) device array printed through a T-shaped pattern design. Leakage current lower than 2 pA (10 V) has certain reference value for improving the yield of short channel device array [1].

When the channel length of a TFT device is reduced to a few micrometers, a short channel effect [112], also known as a "penetration effect", occurs due to unsaturated SD currents, threshold voltage drift, subthreshold swing decrease, and off-state currents increase in the saturation region [109], [113], [114]. The most effective way to reduce the short channel effect is to design the TFT device according to the size rule, that is, the channel width, operating voltage, and dielectric layer thickness need to be reduced by a corresponding multiple of the channel length. The reduction in dielectric layer thickness requires that the electrode thickness be reduced to prevent gate leakage or circuit shorting. Therefore, elimination of short channel effects often requires comprehensive consideration of various layers of materials, processes, and device integration.

A.3. THICKNESS UNIFORMITY

The minimization of the resistivity of inkjet printed electrodes is a major goal of their use in TFT devices [16]. Increasing the depth-to-width ratio of the conductive lines is one of the main approaches. However, this conflicts with the multilayer stack structure of capacitors and TFTs. A thicker electrode causes a larger electric field and reduces the breakdown voltage of the device. Therefore, TFT device electrodes are often required to be thin to reduce the thickness of

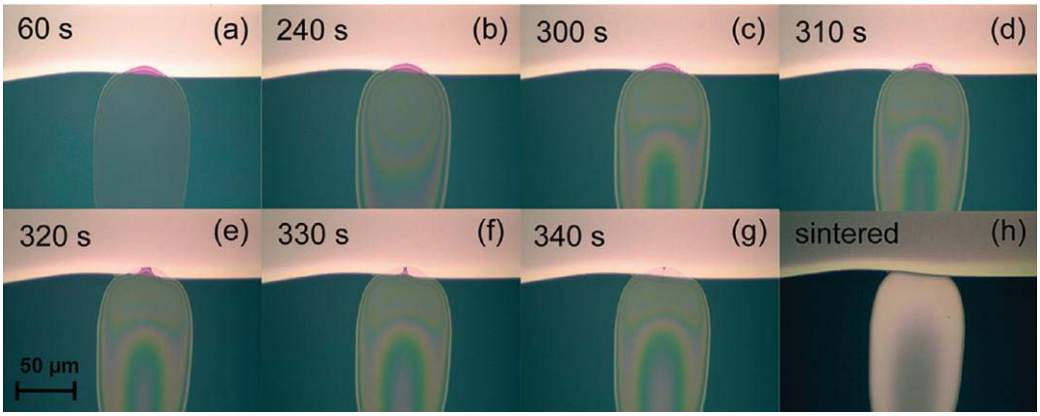

FIGURE 7. **High-yield self-alignment design method for short-channel device array inkjet printing. Copyright 2010 American Chemical Society.**

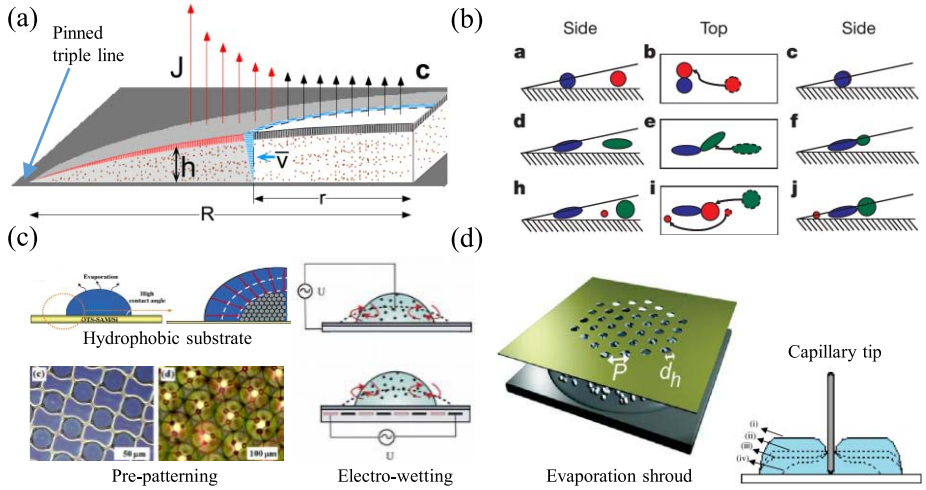

FIGURE 8. **(a) Schematic of the coffee ring effect. Its solutions: (b) particle size and shape change; (c) substrate processing; (d) introduction of ancillary equipment.**

the dielectric layer and the operating voltage, but too thin electrodes can cause high parasitic resistance, thus the thickness of the printed electrodes should only be reduced in the negligible range of parasitic resistance. Thickness control is very important for printing, while non-uniform thickness will cause large local electric field, and reduce the breakdown voltage.

For non-contact inkjet printing, the large-scale uniformity of the film preparation (mainly considering the pattern thickness) is affected by the drying process, due to the low viscosity of the ink and the coffee ring effect [115]. As shown in Fig. 8a, the solvent evaporation near the pinned edge of the droplet is much larger than the volume loss of the liquid, thus the solvent is replenished from the center region to the edge, forming an outward capillary flow, and the solute gathered at the edges to form a coffee ring. Researchers have discovered a variety of coffee ring effect regulation methods in various processes by changing ink composition, substrate status, and adding special equipment: a) Regulation of ink chemistry and composition, such as the addition of surfactants [116]–[119], dodecanethiol [120], high boiling point low surface tension solvents [121], [122], polymer gels [123], or even changes the shape of solutes [124] (Fig. 8b); b) Substrate treatment (Fig. 8c), such as surface hydrophobicity [125], substrate cooling (17 °C) [126], pre-patterning [127] and electrowetting [128]; c) Auxiliary equipment (Fig. 8d), such as a evaporation shroud with micro-holes [129] and capillary tip immersed in drops [130]; d) Rapid curing, such as reducing the curing time by applying a photonic sintering technique to milliseconds or even microseconds.

Although there are many coffee ring regulation methods, not all of them can be used for TFT electrodes morphology control. For example, printing a suitable image on a hydrophobic substrate can be more difficult. Therefore, an appropriate morphology control method must also take into account various factors such as droplet deposition conditions, device structures and performance requirements. Ning *et al.* innovatively proposes a drying micro-environment method to regulate the morphology of printed films [131]. By controlling the surface solvent diffusion concentration

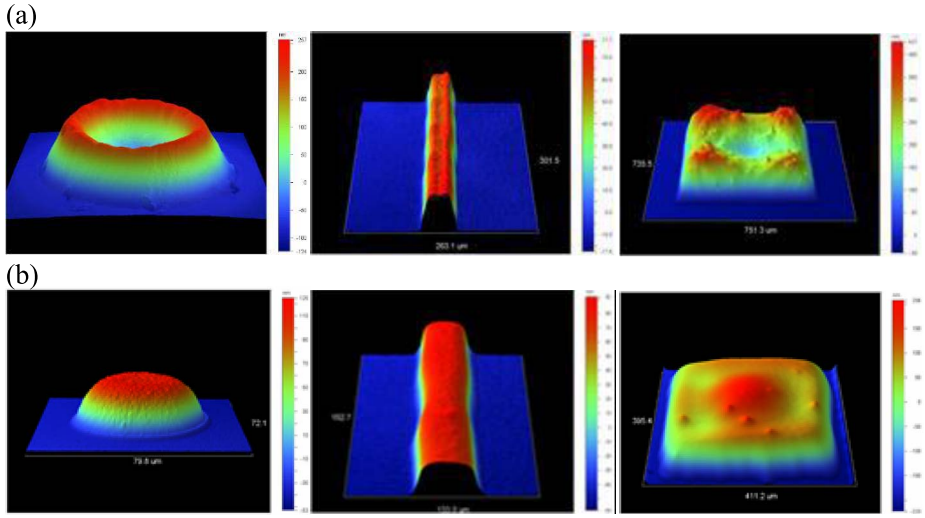

FIGURE 9. Surface profiles of nanoparticles film (a) before, and (b) after optimization of the drying micro-environment.

during the curing process of the wet film, the shape of the printed film can be continuously adjusted from the concave shape to the convex shape. Moreover, dots, lines, and films with smooth surfaces can be all obtained (Fig. 9).

A.4. HIGH ADHESION FILM PREPARATION

Silver nanoparticles ink is the most commonly used conductive ink, and its resistivity can be as low as several μΩ·cm, but its adhesiveness restricts its application in the manufacture of flexible electronic devices. Adhesion is generally improved in three ways: (1) Adding an adhesive to achieve a balance of adhesion and conductivity; (2) Inserting a low glass transition temperature (T_g) polymer interface layer, and strong melting will occur when the sintering temperature is above its T_g [132], [133]; (3) Surface energy matching with optimized silver/substrate interface by inserting a interface layer between them [133].

B. HIGH-PERFORMANCE TFT ELECTRODES INKJET PRINTING

B.1. CONTACT CHARACTERISTICS

Schematic of High-performance TFT electrodes inkjet printing is shown in Fig. 10. The fast operation of the device can reduce the requirement for the graphic technology of inkjet printing equipment through the increase of carrier mobility. For traditional inkjet printing technology, TFT mobility greater than 10 $cm^2V^{-1}s^{-1}$ is a key indicator for achieving high resolution display. The relationship between the effective mobility of the device saturation region and the semiconductor intrinsic mobility can be expressed as follows:

$$\mu_{eff} = \frac{L\mu_0}{L + \mu_0 C_i W R_C (V_{GS} - V_{TH})} \tag{8}$$

μ_{eff}, effective mobility in the saturated region of the device; μ_0, semiconductor intrinsic mobility; C_i, gate dielectric capacitance per unit area; R_C, contact resistance; L, channel length; W, channel width; V_{GS}, gate-source voltage; V_{TH}, threshold voltage.

From Equation (8), we can see that the increasing of the effective mobility in the saturation region of the device can be achieved by increasing the channel length L, the semiconductor intrinsic mobility μ_0, the gate dielectric capacitance per unit area, C_i, and by reducing the channel width W and the contact resistance R_C. However, above methods are not all applicable to the realization of large size, high resolution display.

When the channel length L is large enough, the effective mobility and semiconductor intrinsic mobility tend to be consistent; as L decreases, the effective mobility will become smaller and smaller [134], [135]. The larger the contact resistance R_C, the more the effective mobility decreases with the decreasing of the channel length. However, as can be seen from Equations (5) and (6), increasing the channel length L actually decreases the cutoff frequency f_T and the SD currents I_D. Decreasing the channel width W actually decreases the SD currents I_D, and finally makes the drive capability or operating speed of the TFT reduced. It should not be used as a means of regulating the effective mobility, nor is it detrimental to the minimization and high-level integration of printed electronics. Increasing the semiconductor intrinsic mobility μ_0, the gate dielectric capacitance per unit area C_i, and decreasing the contact resistance R_C are effective ways to increase the effective mobility and eventually achieve high performance TFT. The first two factors are the preconditions for high performance TFT with inkjet printed electrodes, which has a lot to do with the selection of high performance semiconductors and insulation layers. The contact resistance is an important index that must be controlled in the inkjet printing process.

The interface between the inkjet printed electrodes and the semiconductor layer can be improved in a plurality of ways: 1) Most of the contact resistance is caused by

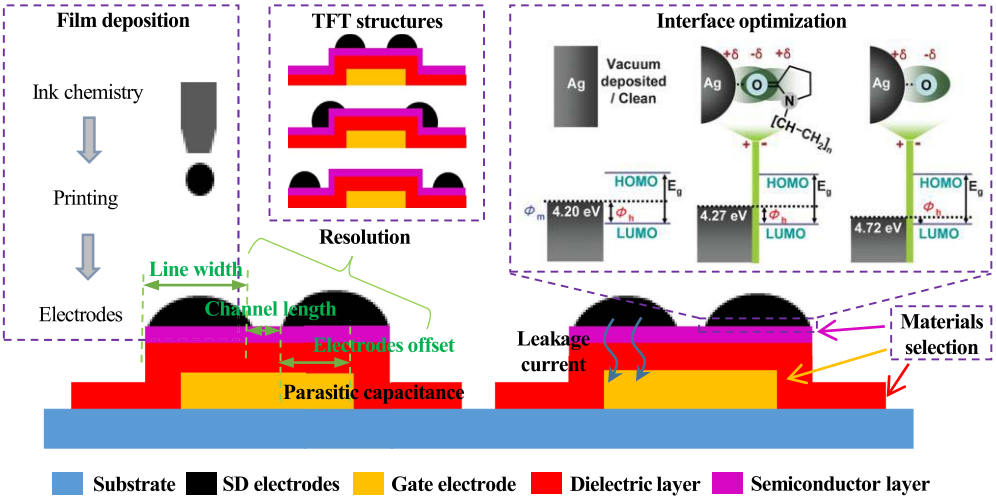

FIGURE 10. High-performance TFT electrodes inkjet printing (materials selection, film deposition, interface optimization and TFT structures). The inserted picture for interface optimization shows the changing of chemical state of the ligands on the surface of the metal nanoparticles to change their work function. Copyright 2008 WILEY-VCH Verlag GmbH & Co. KGaA, Weinheim.

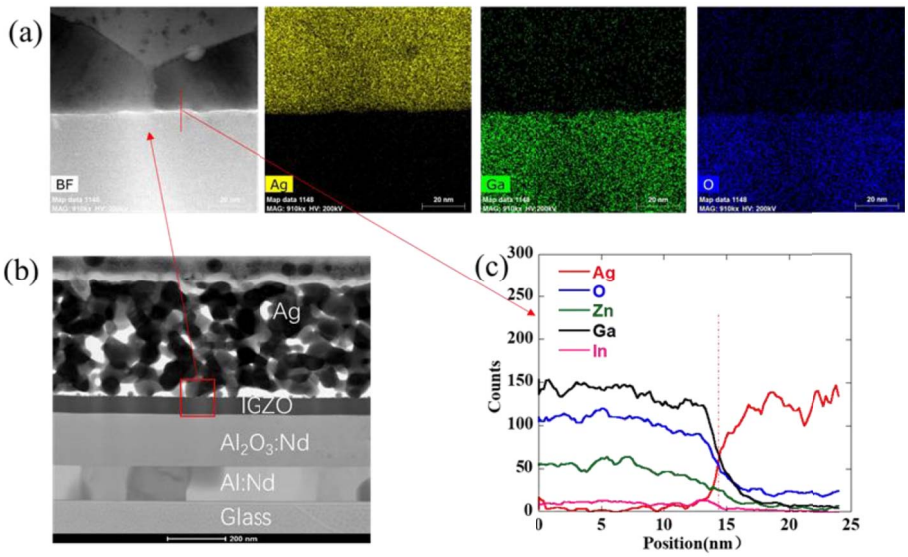

FIGURE 11. TEM measurements of a-IGZO TFT with Inkjet printed silver electrodes: (a) EDS mapping; (b) Cross section of TFT (c) EDS line scanning.

an energy barrier existing between the electrodes and the semiconductor layer, thus a suitable semiconductor material should be selected [136], [137]; 2) Regulate the carrier concentration semiconductor layer by optimizing the deposition process [138], [139]; 3) Change the thickness of the printed electrodes, and adjust their work function to a certain extent [140]; 4) Suitable substrate deposition temperature and post-annealing processes to control the barrier and interface defect states of the interfacial carbon layer [141], [142]; 5) Inserting a surface modification layer between the electrodes and the semiconductor [143]–[147]; 6) Interfacial plasma treatment [148]; 7) Using a suitable annealing process to change the chemical state of the ligands on the surface of the metal nanoparticles to change their work function [149] (inserted picture in Fig. 10 for interface optimization); 8) Improve the wettability [143] and the standard electrode potential [150] of the electrodes materials.

Ning *et al.* reduced the Ag/IGZO interface carbon residue by optimizing the inkjet printing film deposition process [142], [151]. The contact resistance of the device is 81.8 Ω·m. The optimized TFT device has the mobility of 6.23 $cm^2/V{\cdot}s$, the switching ratio of 6.85×10^7, the subthreshold swing of 0.37 V/decade, and the turn on voltage of 0.88 V. Transmission electron microscopy (TEM) was used to analyze the interfacial contact between inkjet printed silver electrodes and semiconductor layer. As shown in Fig. 11, the inkjet printed silver electrodes are formed in a conductive network shape with a uniform thickness and good contact with the IGZO semiconductor layer. The interface was clear and free of impurities, and there is no diffusion or erosion

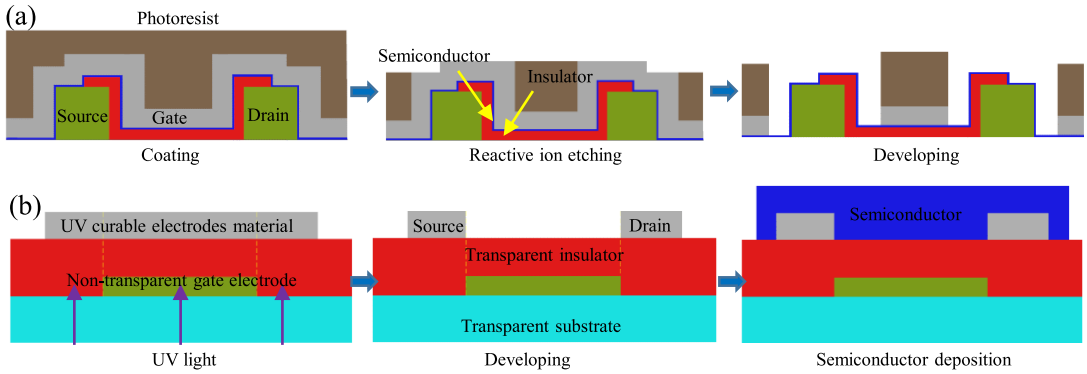

FIGURE 12. **Preparation of self-aligned TFT structure based on (a) photolithography process, and (b) UV irradiation.**

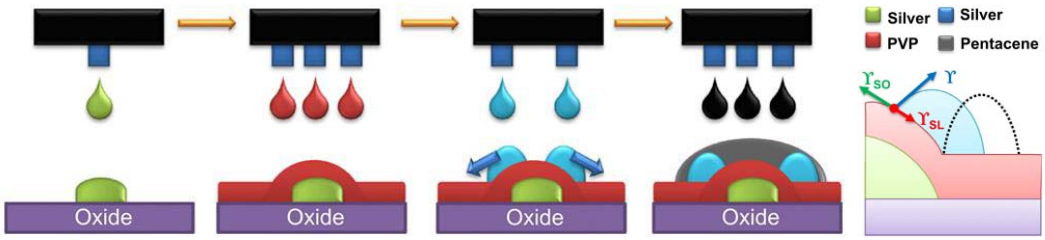

FIGURE 13. **Preparation of self-aligned TFT structure based on substrate wettability. Copyright 2010 Elsevier B.V. Published by Elsevier B.V. All rights reserved.**

occurred. It was proved that the inkjet printed silver films can be used as source and drain electrodes in a thin film transistor. Considering various factors in the inkjet printing processes of TFTs, the introduction of suitable SAMs is the most effective method to improve the interface, which can simultaneously achieve various purposes such as improving the mobility, switching ratio, etc., thereby realizing high efficiency and energy saving of TFT devices [7].

B.2. STRUCTURES OF PRINTED TFTS

Due to the limited accuracy of conventional inkjet printing equipment, printed TFTs generally have poor device performance due to materials, channel length, and very high parasitic capacitance (SD electrodes overlap the gate electrode >10 μm) [24], [152]. It is possible to achieve high device mobility by breaking through the limitations of materials [153], while introducing self-aligned printing technologies can achieve channel lengths of 100 nm [95], [109], [110]. However, the alignment accuracy of multiple layers is still the bottleneck of the printing technology. The overlapping of gate electrode and the SD electrodes of TFT device will affect the performance: 1) It causes parasitic capacitance and reduces the device operating speed; 2) The leakage current will be increased due to the presence of ink solvents and additives, and the increasing of overlapping areas [154]. To overcome the above drawbacks, preparation of self-aligned TFT devices is particularly important.

Self-aligned TFT devices usually require photolithographic techniques [109], [155], [156]. In a high aspect ratio electrode printing technique, the gate electrode thickness can be used to control the offset length between the gate electrode and the SD electrodes more accurately (Fig. 12a). As the offset length increases, leakage current will be reduced accordingly [154]. For the conductive inks, which can be UV cured and sintered to obtain high performance, the SD electrodes of non-overlapped portions of the gate can be selectively cured to achieve self-alignment purposes (Fig. 12b).

In the preparation of self-aligned TFT devices, the use of photolithography process, although with high precision, will increase the cost. Moreover, the development process can damage the back channel of the active materials and is not suitable for stretchable flexible substrates. Based on the above conditions, the self-alignment of the TFT SD electrodes with respect to the gate electrode can be achieved by a substrate wetting based slide down process (Fig. 13), thus no photolithography and vacuum processes is needed. The process can realize a minimum overlap distance of 0.47 μm between the SD electrodes and the gate electrode [157].

Since inkjet printing is a solution-based thin film deposition process, there is more selectivity in terms of materials. Ionic gels [17], [29], [158], a solid electrolyte-type gate dielectric material, can form an electric double-layer structure at the electrode-electrolyte/semiconductor-electrolyte interface in 10 μs time scale. The capacitance of these nano-sized double layers are very large (usually greater than 1 μFcm^{-2}), which can lower the turn on voltage of TFT. In addition, the high polarization of the gate dielectric layer

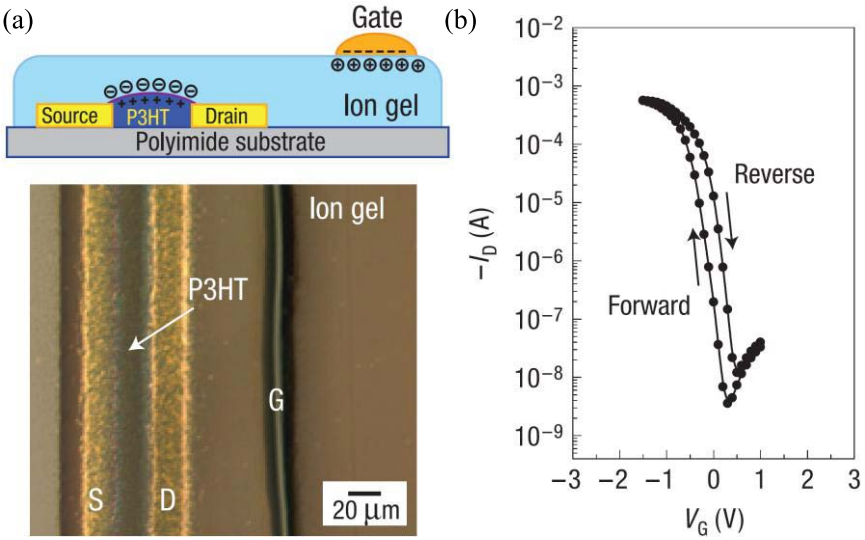

FIGURE 14. **Schematic of the physical compensation of the channel region of the ion gel TFT and its device optical photo; (2) TFT transfer characteristic curve. Copyright 2008 Macmillan Publishers Limited. All rights reserved.**

makes the gate electrode and the channel region form a physical compensation, so that gate electrode and SD electrodes with a certain amount of offset are automatically aligned to ensure low leakage and high switching speed [23] (Fig. 14). Since this process requires only the replacement of the gate dielectric materials and does not add any additional processes, it is valuable for printed TFTs with high performance by using ion gel as insulator layers.

IV. CONCLUSION

In summary, with the continuous development of equipment, materials, and processes in inkjet printing, as well as the understanding of their interaction mechanisms, inkjet printed electrodes have made important progress in terms of printability, high conductivity, high precision, high adhesion and low contact resistance, and are extremely important for the realization of high resolution, high performance, and flexible TFT devices. In spite of this, many aspects still need to be further studied: 1) Equipment with higher precision, more stability, and lower requirements for materials (viscosity and electrical properties); 2) The preparation of more electrodes ink materials with high performance, such copper inks, which require lower processing temperature; 3) Lower cost, more simplified processes, and higher yields of high resolution, high performance TFTs. By combining the advantages of inkjet printing technology with the constant innovation of materials and processes, the application of inkjet printed electrodes for TFT devices is bound to have a bright future.

REFERENCES

[1] M. Caironi, E. Gili, T. Sakanoue, X. Cheng, and H. Sirringhaus, "High yield, single droplet electrode arrays for nanoscale printed electronics," *ACS Nano*, vol. 4, no. 3, pp. 1451–1456, 2010.

[2] D. J. Finn, M. Lotya, and J. N. Coleman, "Inkjet printing of silver nanowire networks," *ACS Appl. Mater. Interfaces*, vol. 7, no. 17, pp. 9254–9261, May 2015.

[3] Y.-T. Kwon, Y.-I. Lee, K.-J. Lee, Y.-M. Choi, and Y.-H. Choa, "A novel method for fine patterning by piezoelectrically induced pressure adjustment of inkjet printing," *J. Elect. Mater.*, vol. 44, no. 8, pp. 2608–2614, 2015.

[4] M. Mashayekhi *et al.*, "Inkjet printing design rules formalization and improvement," *J. Display Technol.*, vol. 11, no. 8, pp. 658–665, Aug. 2015.

[5] A. Chiolerio *et al.*, "Hybrid Ag-based inks for nanocomposite inkjet printed lines: RF properties," *J. Alloys Compd.*, vol. 615, pp. S501–S504, Dec. 2014.

[6] J. Niittynen *et al.*, "Alternative sintering methods compared to conventional thermal sintering for inkjet printed silver nanoparticle ink," *Thin Solid Films*, vol. 556, pp. 452–459, Apr. 2014.

[7] T. Wei *et al.*, "Inkjet printed fine silver electrodes for all-solution-processed low-voltage organic thin film transistors," *J. Mater. Chem. C*, vol. 2, no. 11, pp. 1995–2000, 2014.

[8] V. Bromberg, S. Ma, and T. J. Singler, "High-resolution inkjet printing of electrically conducting lines of silver nanoparticles by edge-enhanced twin-line deposition," *Appl. Phys. Lett.*, vol. 102, no. 21, 2013, Art. no. 214101.

[9] Z. Zhang *et al.*, "Controlled inkjetting of a conductive pattern of silver nanoparticles based on the coffee-ring effect," *Adv. Mater.*, vol. 25, no. 46, pp. 6714–6718, 2013.

[10] B.-J. De Gans, P. C. Duineveld, and U. S. Schubert, "Inkjet printing of polymers: State of the art and future developments," *Adv. Mater.*, vol. 16, no. 3, pp. 203–213, 2004.

[11] B. Kang, W. H. Lee, and K. Cho, "Recent advances in organic transistor printing processes," *ACS Appl. Mater. Interfaces*, vol. 5, no. 7, pp. 2302–2315, 2013.

[12] V. Subramanian *et al.*, "High-speed printing of transistors: From inks to devices," *Proc. IEEE*, vol. 103, no. 4, pp. 567–582, Apr. 2015.

[13] S. Mishra, K. Barton, and A. Alleyne, "Control of high-resolution electrohydrodynamic jet printing," in *Proc. Amer. Control Conf.*, Baltimore, MD, USA, 2010, pp. 6537–6542.

[14] Y. Kim, S. Jang, and J. H. Oh, "High-resolution electrohydrodynamic printing of silver nanoparticle ink via commercial hypodermic needles," *Appl. Phys. Lett.*, vol. 106, no. 1, Jan. 2015, Art. no. 014103.

[15] J. Park and J. Hwang, "Fabrication of a flexible Ag-grid transparent electrode using AC based electrohydrodynamic jet printing," *J. Phys. D Appl. Phys.*, vol. 47, no. 40, 2014, Art. no. 405102.

[16] A. Mahajan, C. D. Frisbie, and L. F. Francis, "Optimization of aerosol jet printing for high-resolution, high-aspect ratio silver lines," *ACS Appl. Mater. Interfaces*, vol. 5, no. 11, pp. 4856–4864, Jun. 2013.

[17] K. Hong, S. H. Kim, A. Mahajan, and C. D. Frisbie, "Aerosol jet printed p- and n-type electrolyte-gated transistors with a variety of electrode materials: Exploring practical routes to printed electronics," *ACS Appl. Mater. Interfaces*, vol. 6, no. 21, pp. 18704–18711, Nov. 2014.

[18] R. Liu *et al.*, "All-carbon-based field effect transistors fabricated by aerosol jet printing on flexible substrates," *J. Micromechan. Microeng.*, vol. 23, no. 6, 2013, Art. no. 065027.

[19] Y. Pan, Y. Huang, L. Guo, Y. Ding, and Z. Yin, "Addressable multi-nozzle electrohydrodynamic jet printing with high consistency by multi-level voltage method," *AIP Adv.*, vol. 5, no. 4, 2015, Art. no. 0471084.

[20] J. Lee *et al.*, "Design and evaluation of a silicon based multi-nozzle for addressable jetting using a controlled flow rate in electrohydrodynamic jet printing," *Appl. Phys. Lett.*, vol. 93, no. 24, 2008, Art. no. 243114.

[21] K. Murata, "Ultrafine fluid jet apparatus," U.S. Patent US 7 434 912 B2, 2008.

[22] M. Laurila, "Super inkjet printed redistribution layer for a MEMS device," M.S. thesis, Dept. Electron. Commun. Eng., Tampere Univ. Technol., Tampere, Finland, 2015.

[23] J. H. Cho *et al.*, "Printable ion-gel gate dielectrics for low-voltage polymer thin-film transistors on plastic," *Nat. Mater.*, vol. 7, no. 11, pp. 900–906, Nov. 2008.

[24] H. Yan *et al.*, "A high-mobility electron-transporting polymer for printed transistors," *Nature*, vol. 457, no. 7230, pp. 679–686, Feb. 2009.

[25] S.-K. Lee *et al.*, "Stretchable graphene transistors with printed dielectrics and gate electrodes," *Nano Lett.*, vol. 11, no. 11, pp. 4642–4646, 2011.

[26] S. Wang, M. Ha, M. Manno, C. D. Frisbie, and C. Leighton, "Hopping transport and the hall effect near the insulator–metal transition in electrochemically gated poly(3-hexylthiophene) transistors," *Nat. Commun.*, vol. 3, no. 1, p. 1210, 2012.

[27] J. Zhao, Y. Gao, J. Lin, Z. Chen, and Z. Cui, "Printed thin-film transistors with functionalized single-walled carbon nanotube inks," *J. Mater. Chem.*, vol. 22, no. 5, pp. 2051–2056, 2012.

[28] J. Zhao *et al.*, "Fabrication and electrical properties of all-printed carbon nanotube thin film transistors on flexible substrates," *J. Mater. Chem.*, vol. 22, no. 38, 2012. Art. no. 20747.

[29] S. H. Kim, K. Hong, K. H. Lee, and C. D. Frisbie, "Performance and stability of aerosol-jet-printed electrolyte-gated transistors based on poly(3-hexylthiophene)," *ACS Appl. Mater. Interfaces*, vol. 5, no. 14, pp. 6580–6585, 2013.

[30] Z. Liu *et al.*, "Effect of surface wettability properties on the electrical properties of printed carbon nanotube thin-film transistors on SiO2 /Si substrates," *ACS Appl. Mater. Interfaces*, vol. 6, no. 13, pp. 9997–10004, Jul. 2014.

[31] W. Xu *et al.*, "Sorting of large-diameter semiconducting carbon nanotube and printed flexible driving circuit for organic light emitting diode (OLED)," *Nanoscale*, vol. 6, no. 3, pp. 1589–1595, 2014.

[32] X. Wu *et al.*, "Printable poly(methylsilsesquioxane) dielectric ink and its application in solution processed metal oxide thin-film transistors," *RSC Adv.*, vol. 5, no. 27, pp. 20924–20930, 2015.

[33] C. Cao, J. B. Andrews, and A. D. Franklin, "Completely printed, flexible, stable, and hysteresis-free carbon nanotube thin-film transistors via aerosol jet printing," *Adv. Elect. Mater.*, vol. 3, no. 5, 2017, Art. no. 1700057.

[34] B. Derby and N. Reis, "Inkjet printing of highly loaded particulate suspensions," *MRS Bull.*, vol. 28, no. 11, pp. 815–818, 2003.

[35] N. Reis, C. Ainsley, and B. Derby, "Ink-jet delivery of particle suspensions by piezoelectric droplet ejectors," *J. Appl. Phys.*, vol. 97, no. 9, pp. 1–6, 2005.

[36] D. Jang, D. Kim, and J. Moon, "Influence of fluid physical properties on ink-jet printability," *Langmuir*, vol. 25, no. 5, pp. 2629–2635, 2009.

[37] F. Xue, Y. Su, and K. Varahramyan, "Modified PEDOT-PSS conducting polymer as S/D electrodes for device performance enhancement of P3HT TFTs," *IEEE Trans. Electron Devices*, vol. 52, no. 9, pp. 1982–1987, Sep. 2005.

[38] F. Torrisi *et al.*, "Inkjet-printed graphene electronics," *ACS Nano*, vol. 6, no. 4, pp. 2992–3006, 2012.

[39] S. Park, M. Vosguerichian, and Z. Bao, "A review of fabrication and applications of carbon nanotube film-based flexible electronics," *Nanoscale*, vol. 5, no. 5, pp. 1727–1752, 2013.

[40] A. Kamyshny and S. Magdassi, "Conductive nanomaterials for printed electronics," *Small*, vol. 10, no. 17, pp. 3515–3535, 2014.

[41] S. Magdassi, A. Bassa, A. Y. Vinetsky, and A. Kamyshny, "Silver nanoparticles as pigments for water-based ink-jet inks," *Chem. Mater.*, vol. 15, no. 11, pp. 2208–2217, 2003.

[42] A. Kamyshny, "Metal-based inkjet inks for printed electronics," *Open Appl. Phys. J.*, vol. 4, no. 19, pp. 19–36, 2011.

[43] S. Norita *et al.*, "Inkjet-printed copper electrodes using photonic sintering and their application to organic thin-film transistors," *Org. Electron.*, vol. 25, pp. 131–134, Oct. 2015.

[44] H. Meier, U. Löffelmann, D. Mager, P. J. Smith, and J. G. Korvink, "Inkjet printed, conductive, 25 μm wide silver tracks on unstructured polyimide," *Physica Status Solidi (A)*, vol. 206, no. 7, pp. 1626–1630, 2009.

[45] B. J. Perelaer, A. W. M. de Laat, C. E. Hendriks, and U. S. Schubert, "Inkjet-printed silver tracks: Low temperature curing and thermal stability investigation," *J. Mater. Chem.*, vol. 18, no. 27, p. 3209, 2008.

[46] H. H. Lee, K. S. Chou, and K. C. Huang, "Inkjet printing of nanosized silver colloids," *Nanotechnology*, vol. 16, no. 10, pp. 2436–2441, 2005.

[47] A. Kamyshny, "Metal-based Inkjet inks for printed electronics," *Open Appl. Phys. J.*, vol. 4, no. 19, pp. 19–36, 2011.

[48] J. Mewis and N. J. Wagner, *Colloidal Suspension Rheology*. Cambridge, U.K.: Cambridge Univ. Press, 2013.

[49] R. G. Larson, *The Structure and Rheology of Complex Fluid*. New York, NY, USA: Oxford Univ. Press, 1998.

[50] A. L. Dearden *et al.*, "A low curing temperature silver ink for use in ink-jet printing and subsequent production of conductive tracks," *Macromol. Rapid Commun.*, vol. 26, no. 4, pp. 315–318, 2005.

[51] K. F. Teng and R. W. Vest, "Metallization of solar cells with ink jet printing and silver metallo-organic inks," *IEEE Trans. Compon., Hybrids, Manuf. Technol.*, vol. 11, no. 3, pp. 291–297, Sep. 1988.

[52] S. Jeong, H. C. Song, W. W. Lee, Y. Choi, and B. Ryu, "Preparation of aqueous Ag ink with long-term dispersion stability and its inkjet printing for fabricating conductive tracks on a polyimide film," *J. Appl. Phys.*, vol. 108, no. 10, 2010, Art. no. 102805.

[53] H. S. Koo *et al.*, "Fabrication and chromatic characteristics of the greenish LCD colour-filter layer with nano-particle ink using inkjet printing technique," *Displays*, vol. 27, no. 3, pp. 124–129, 2006.

[54] H. W. Choi, T. Zhou, M. Singh, and G. E. Jabbour, "Recent developments and directions in printed nanomaterials," *Nanoscale*, vol. 7, no. 8, pp. 3338–3355, 2014.

[55] S. Gamerith *et al.*, "Direct ink-jet printing of Ag–Cu nanoparticle and Ag-precursor based electrodes for OFET applications," *Adv. Funct. Mater.*, vol. 17, no. 16, pp. 3111–3118, 2007.

[56] Y. Takeda *et al.*, "Integrated circuits using fully solution-processed organic TFT devices with printed silver electrodes," *Org. Electron.*, vol. 14, no. 12, pp. 3362–3370, 2013.

[57] M. Allen *et al.*, "Contactless electrical sintering of silver nanoparticles on flexible substrates," *IEEE Trans. Microw. Theory Techn.*, vol. 59, no. 5, pp. 1419–1429, May 2011.

[58] D. Tobjörk *et al.*, "IR-sintering of ink-jet printed metal-nanoparticles on paper," *Thin Solid Films*, vol. 520, no. 7, pp. 2949–2955, 2012.

[59] E. M. Hamad *et al.*, "Inkjet printing of UV-curable adhesive and dielectric inks for microfluidic devices," *Lab Chip*, vol. 16, no. 1, pp. 70–74, Jan. 2016.

[60] M. H. A. van Dongen, A. van Loon, R. J. Vrancken, J. P. C. Bernards, and J. F. Dijksman, "UV-mediated coalescence and mixing of inkjet printed drops," *Exp. Fluids*, vol. 55, no. 5, p. 1744, 2014.

[61] K. C. Yung, X. Gu, C. P. Lee, and H. S. Choy, "Ink-jet printing and camera flash sintering of silver tracks on different substrates," *J. Mater. Process. Technol.*, vol. 210, no. 15, pp. 2268–2272, 2010.

[62] A. J. Lopes, I. H. Lee, E. MacDonald, R. Quintana, and R. Wicker, "Laser curing of silver-based conductive inks for in situ 3D structural electronics fabrication in stereolithography," *J. Mater. Process. Technol.*, vol. 214, no. 9, pp. 1935–1945, 2014.

[63] I. Theodorakos, F. Zacharatos, R. Geremia, D. Karnakis, and I. Zergioti, "Selective laser sintering of Ag nanoparticles ink for applications in flexible electronics," *Appl. Surface Sci.*, vol. 336, pp. 157–162, May 2015.

[64] M. Makrygianni, I. Kalpyris, C. Boutopoulos, and I. Zergioti, "Laser induced forward transfer of Ag nanoparticles ink deposition and characterization," *Appl. Surface Sci.*, vol. 297, pp. 40–44, Apr. 2014.
[65] A. Chiolerio *et al.*, "Inkjet printing and low power laser annealing of silver nanoparticle traces for the realization of low resistivity lines for flexible electronics," *Microelectron. Eng.*, vol. 88, no. 8, pp. 2481–2483, 2011.
[66] J. Perelaer, B.-J. de Gans, and U. S. Schubert, "Ink-jet printing and microwave sintering of conductive silver tracks," *Adv. Mater.*, vol. 18, no. 16, pp. 2101–2104, Aug. 2006.
[67] T. Minari *et al.*, "Room-temperature printing of organic thin-film transistors with π-junction gold nanoparticles," *Adv. Funct. Mater.*, vol. 24, no. 31, pp. 4886–4892, 2014.
[68] I. E. Stewart, M. J. Kim, and B. J. Wiley, "Effect of morphology on the electrical resistivity of silver nanostructure films," *ACS Appl. Mater. Interfaces*, vol. 9, no. 2, pp. 1870–1876, 2017.
[69] Z. Liu, Y. Su, and K. Varahramyan, "Inkjet-printed silver conductors using silver nitrate ink and their electrical contacts with conducting polymers," *Thin Solid Films*, vol. 478, nos. 1–2, pp. 275–279, 2005.
[70] T. Y. Dong *et al.*, "One-step synthesis of uniform silver nanoparticles capped by saturated decanoate: Direct spray printing ink to form metallic silver films," *Phys. Chem. Chem. Phys.*, vol. 11, no. 29, pp. 6269–6275, Aug. 2009.
[71] M. Vaseem, K. M. Lee, A. R. Hong, and Y. B. Hahn, "Inkjet printed fractal-connected electrodes with silver nanoparticle ink," *ACS Appl. Mater. Interfaces*, vol. 4, no. 6, pp. 3300–3307, Jun. 2012.
[72] Y.-L. Tai, Y.-X. Wang, Z.-G. Yang, and Z-Q. Chai, "Green approach to prepare silver nanoink with potentially high conductivity for printed electronics," *Surface Interface Anal.*, vol. 43, no. 12, pp. 1480–1485, 2011.
[73] Y. L. Tai and Z. G. Yang, "Facile and scalable preparation of solid silver nanoparticles (<10 nm) for flexible electronics," *ACS Appl. Mater. Interfaces*, vol. 7, no. 31, pp. 17104–17111, Aug. 2015.
[74] J.-T. Wu, S. L.-C. Hsu, M.-H. Tsai, and W.-S. Hwang, "Inkjet printing of low-temperature cured silver patterns by using AgNO3/1-dimethylamino-2-propanol inks on polymer substrates," *J. Phys. Chem. C*, vol. 115, no. 22, pp. 10940–10945, Jun. 2011.
[75] M. Vaseem, G. McKerricher, and A. Shamim, "Robust design of a particle-free silver-organo-complex ink with high conductivity and inkjet stability for flexible electronics," *ACS Appl. Mater. Interfaces*, vol. 8, no. 1, pp. 177–186, Jan. 2016.
[76] K. S. Bhat, R. Ahmad, Y. Wang, and Y.-B. Hahn, "Low-temperature sintering of highly conductive silver ink for flexible electronics," *J. Mater. Chem. C*, vol. 4, no. 36, pp. 8522–8527, 2016.
[77] S. B. Walker and J. A. Lewis, "Reactive silver inks for patterning high-conductivity features at mild temperatures," *J. Amer. Chem. Soc.*, vol. 134, no. 3, pp. 1419–1421, Jan. 2012.
[78] X. Nie, H. Wang, and J. Zou, "Inkjet printing of silver citrate conductive ink on PET substrate," *Appl. Surface Sci.*, vol. 261, pp. 554–560, Nov. 2012.
[79] Y. Dong *et al.*, "Facile synthesis of high silver content MOD ink by using silver oxalate precursor for inkjet printing applications," *Thin Solid Films*, vol. 589, pp. 381–387, Aug. 2015.
[80] P. Buffat and J.-P. Borel, "Size effect on the melting temperature of gold particles," *Phys. Rev. A*, vol. 13, no. 6, pp. 2287–2298, 1976.
[81] K. Dick, T. Dhanasekaran, Z. Zhang, and M. Dan, "Size-dependent melting of silica-encapsulated gold nanoparticles," *J. Amer. Chem. Soc.*, vol. 124, no. 10, p. 2312, 2002.
[82] H. Ning *et al.*, "UV-cured inkjet-printed silver gate electrode with low electrical resistivity," *Nanoscale Res. Lett.*, vol. 12, no. 1, p. 546, 2017.
[83] D. Wakuda, M. Hatamura, and K. Suganuma, "Novel method for room temperature sintering of Ag nanoparticle paste in air," *Chem. Phys. Lett.*, vol. 441, nos. 4–6, pp. 305–308, 2007.
[84] D. Wakuda, K.-S. Kim, and K. Suganuma, "Room-temperature sintering process of Ag nanoparticle paste," *IEEE Trans. Compon. Packag. Technol.*, vol. 32, no. 3, pp. 627–632, Sep. 2009.
[85] S. Magdassi, M. Grouchko, O. Berezin, and A. Kamyshny, "Triggering the sintering of silver nanoparticles at room temperature," *ACS Nano*, vol. 4, no. 4, pp. 1943–1948, Apr. 2010.
[86] M. Grouchko, A. Kamyshny, C. F. Mihailescu, D. F. Anghel, and S. Magdassi, "Conductive inks with a 'built-in' mechanism that enables sintering at room temperature," *ACS Nano*, vol. 5, no. 4, pp. 3354–3359, Apr. 2011.
[87] M. Layani, M. Grouchko, S. Shemesh, and S. Magdassi, "Conductive patterns on plastic substrates by sequential inkjet printing of silver nanoparticles and electrolyte sintering solutions," *J. Mater. Chem.*, vol. 22, no. 29, pp. 14349–14352, 2012.
[88] Y. Long *et al.*, "Rapid sintering of silver nanoparticles in an electrolyte solution at room temperature and its application to fabricate conductive silver films using polydopamine as adhesive layers," *J. Mater. Chem.*, vol. 21, no. 13, p. 4875, 2011.
[89] C. N. Chen *et al.*, "Using nanoparticles as direct-injection printing ink to fabricate conductive silver features on a transparent flexible PET substrate at room temperature," *Acta Materialia*, vol. 60, no. 16, pp. 5914–5924, 2012.
[90] C.-H. Choi, E. Allan-Cole, and C.-H. Chang, "Room temperature fabrication and patterning of highly conductive silver features using in situ reactive inks by microreactor-assisted printing," *J. Mater. Chem. C*, vol. 3, no. 28, pp. 7262–7266, 2015.
[91] Z.-K. Kao, Y.-H. Hung, and Y.-C. Liao, "Formation of conductive silver films via inkjet reaction system," *J. Mater. Chem.*, vol. 21, no. 46, pp. 18799–18803, 2011.
[92] J. T. Wu, S. L. C. Hsu, M. H. Tsai, and W. S. Hwang, "Conductive silver patterns via ethylene glycol vapor reduction of ink-jet printed silver nitrate tracks on a polyimide substrate," *Thin Solid Films*, vol. 517, no. 20, pp. 5913–5917, 2009.
[93] H. Koga *et al.*, "A high-sensitivity printed antenna prepared by rapid low-temperature sintering of silver ink," *RSC Adv.*, vol. 6, no. 87, pp. 84363–84368, 2016.
[94] M. A. M. Leenen, V. Arning, H. Thiem, J. Steiger, and R. Anselmann, "Printable electronics: Flexibility for the future," *Physica Status Solidi Appl. Mater.*, vol. 206, no. 206, pp. 588–597, 2009.
[95] N. Zhao *et al.*, "Self-aligned inkjet printing of highly conducting gold electrodes with submicron resolution," *J. Appl. Phys.*, vol. 101, no. 6, 2007, Art. no. 064513.
[96] J. Z. Wang, Z. H. Zheng, H. W. Li, W. T. S. Huck, and H. Sirringhaus, "Dewetting of conducting polymer inkjet droplets on patterned surfaces," *Nat. Mater.*, vol. 3, no. 3, pp. 171–176, 2004.
[97] A. C. Arias *et al.*, "All jet-printed polymer thin-film transistor active-matrix backplanes," *Appl. Phys. Lett.*, vol. 85, no. 15, pp. 3304–3306, 2004.
[98] J. Doggart, Y. Wu, P. Liu, and S. Zhu, "Facile inkjet-printing self-aligned electrodes for organic thin-film transistor arrays with small and uniform channel length," *ACS Appl. Mater. Interfaces*, vol. 2, no. 8, pp. 2189–2192, 2010.
[99] H. Klauk, "Organic thin-film transistors," *Chem. Soc. Rev.*, vol. 39, no. 7, pp. 2643–2666, 2010.
[100] H. K. Huh, S. Jung, K. W. Seo, and S. J. Lee, "Role of polymer concentration and molecular weight on the rebounding behaviors of polymer solution droplet impacting on hydrophobic surfaces," *Microfluidics Nanofluidics*, vol. 18, nos. 5–6, pp. 1221–1232, 2015.
[101] P. C. Duineveld, "The stability of ink-jet printed lines of liquid with zero receding contact angle on a homogeneous substrate," *J. Fluid Mech.*, vol. 477, pp. 175–200, Feb. 2003.
[102] T. Sekitani, Y. Noguchi, U. Zschieschang, H. Klauk, and T. Someya, "Organic transistors manufactured using inkjet technology with sub-femtoliter accuracy," *Proc. Nat. Acad. Sci. USA*, vol. 105, no. 13, pp. 4976–4980, 2008.
[103] J. U. Park *et al.*, "High-resolution electrohydrodynamic jet printing," *Nat. Mater.*, vol. 6, no. 10, pp. 782–789, 2007.
[104] K. Murata, J. Matsumoto, A. Tezuka, Y. Matsuba, and H. Yokoyama, "Super-fine ink-jet printing: Toward the minimal manufacturing system," *Microsyst. Technol. Micro Nanosyst. Inf. Stor. Process. Syst.*, vol. 12, nos. 1–2, pp. 2–7, 2005.
[105] S. H. Ko *et al.*, "Laser based hybrid inkjet printing of nanoink for flexible electronics," in *Proc. SPIE*, vol. 5713, 2005, pp. 97–104.
[106] A. Mahajan *et al.*, "High-resolution, high-aspect ratio conductive wires embedded in plastic substrates," *ACS Appl. Mater. Interfaces*, vol. 7, no. 3, pp. 1841–1847, Jan. 2015.
[107] K. Suzuki *et al.*, "Fabrication of all-printed organic TFT array on flexible substrate," *J. Photopolym. Sci. Technol.*, vol. 24, no. 5, pp. 565–570, 2011.
[108] H. Sirringhaus *et al.*, "High-resolution inkjet printing of all-polymer transistor circuits," *Science*, vol. 290, no. 7, pp. 2123–2126, 2001.
[109] Y.-Y. Noh, N. Zhao, M. Caironi, and H. Sirringhaus, "Downscaling of self-aligned, all-printed polymer thin-film transistors," *Nat. Nanotechnol.*, vol. 2, no. 12, pp. 784–789, Dec. 2007.

[110] C. W. Sele, T. von Werne, R. H. Friend, and H. Sirringhaus, "Lithography-free, self-aligned inkjet printing with sub-hundred-nanometer resolution," *Adv. Mater.*, vol. 17, no. 8, pp. 997–1001, 2005.

[111] H. Ning *et al.*, "Direct patterning of silver electrodes with 2.4 μm channel length by piezoelectric inkjet printing," *J. Colloid Interface Sci.*, vol. 487, pp. 68–72, Feb. 2017.

[112] D. Tu *et al.*, "A static model for electrolyte-gated organic field-effect transistors," *IEEE Trans. Electron Devices*, vol. 58, no. 10, pp. 3574–3582, Oct. 2011.

[113] R. Shiwaku *et al.*, "Control of threshold voltage in organic thin-film transistors by modifying gate electrode surface with MoO_x aqueous solution and inverter circuit applications," *Appl. Phys. Lett.*, vol. 106, no. 5, 2015, Art. no. 053301.

[114] T. Yokota *et al.*, "Low-voltage organic transistor with subfemtoliter inkjet source–drain contacts," *MRS Commun.*, vol. 1, no. 1, pp. 3–6, 2011.

[115] R. D. Deegan *et al.*, "Capillary flow as the cause of ring stains from dried liquid drops," *Nature*, vol. 389, no. 6653, pp. 827–829, 1997.

[116] V. N. Truskett and K. J. Stebe, "Influence of surfactants on an evaporating drop: Fluorescence images and particle deposition patterns," *Langmuir*, vol. 19, no. 20, pp. 8271–8279, 2003.

[117] T. Kajiya, W. Kobayashi, T. Okuzono, and M. Doi, "Controlling the drying and film formation processes of polymer solution droplets with addition of small amount of surfactants," *J. Phys. Chem. B*, vol. 113, no. 47, pp. 15460–15466, Nov. 2009.

[118] T. Still, P. J. Yunker, and A. G. Yodh, "Surfactant-induced Marangoni eddies alter the coffee-rings of evaporating colloidal drops," *Langmuir*, vol. 28, no. 11, pp. 4984–4988, Mar. 2012.

[119] W. Sempels, R. De Dier, H. Mizuno, J. Hofkens, and J. Vermant, "Auto-production of biosurfactants reverses the coffee ring effect in a bacterial system," *Nat. Commun.*, vol. 4, p. 1757, Apr. 2013.

[120] T. P. Bigioni *et al.*, "Kinetically driven self assembly of highly ordered nanoparticle monolayers," *Nat. Mater.*, vol. 5, no. 4, pp. 265–270, Apr. 2006.

[121] D. Kim, S. Jeong, B. K. Park, and J. Moon, "Direct writing of silver conductive patterns: Improvement of film morphology and conductance by controlling solvent compositions," *Appl. Phys. Lett.*, vol. 89, no. 26, 2006, Art. no. 264101.

[122] H. Liu *et al.*, "Line printing solution-processable small molecules with uniform surface profile via ink-jet printer," *J. Colloid Interface Sci.*, vol. 465, pp. 106–111, Mar. 2016.

[123] A. M. J. van den Berg, A. W. M. de Laat, P. J. Smith, J. Perelaer, and U. S. Schubert, "Geometric control of inkjet printed features using a gelating polymer," *J. Mater. Chem.*, vol. 17, no. 7, pp. 677–683, 2007.

[124] P. J. Yunker, T. Still, M. A. Lohr, and A. G. Yodh, "Suppression of the coffee-ring effect by shape-dependent capillary interactions," *Nature*, vol. 476, no. 7360, pp. 308–311, Sep. 2011.

[125] H.-Y. Ko, J. Park, H. Shin, and J. Moon, "Rapid self-assembly of monodisperse colloidal spheres in an ink-jet printed droplet," *Chem. Mater.*, vol. 16, no. 22, pp. 4212–4215, 2004.

[126] D. Soltman and V. Subramanian, "Inkjet-printed line morphologies and temperature control of the coffee ring effect," *Langmuir*, vol. 24, no. 5, pp. 2224–2231, 2008.

[127] I. U. Vakarelski, D. Y. Chan, T. Nonoguchi, H. Shinto, and K. Higashitani, "Assembly of gold nanoparticles into microwire networks induced by drying liquid bridges," *Phys. Rev. Lett.*, vol. 102, no. 5, Feb. 2009, Art. no. 058303.

[128] H. B. Eral, D. M. Augustine, M. H. G. Duits, and F. Mugele, "Suppressing the coffee stain effect: How to control colloidal self-assembly in evaporating drops using electrowetting," *Soft Matter*, vol. 7, no. 10, pp. 4954–4958, 2011.

[129] D. J. Harris, H. Hu, J. C. Conrad, and J. A. Lewis, "Patterning colloidal films via evaporative lithography," *Phys. Rev. Lett.*, vol. 98, no. 14, 2007, Art. no. 148301.

[130] K. Keseroğlu and M. Çulha, "Assembly of nanoparticles at the contact line of a drying droplet under the influence of a dipped tip," *J. Colloid Interface Sci.*, vol. 360, no. 1, pp. 8–14, 2011.

[131] R. Tao *et al.*, "Homogeneous surface profiles of inkjet-printed silver nanoparticle films by regulating their drying microenvironment," *J. Phys. Chem. C*, vol. 121, no. 16, pp. 8992–8998, Apr. 2017.

[132] T. Sekine *et al.*, "Improvement of mechanical durability on organic TFT with printed electrodes prepared from nanoparticle ink," *Appl. Surface Sci.*, vol. 294, pp. 20–23, Mar. 2014.

[133] T. Sekine, K. Fukuda, D. Kumaki, and S. Tokito, "Enhanced adhesion mechanisms between printed nano-silver electrodes and underlying polymer layers," *Nanotechnology*, vol. 26, no. 32, 2015, Art. no. 321001.

[134] F. Ante *et al.*, "Contact resistance and megahertz operation of aggressively scaled organic transistors," *Small*, vol. 8, no. 1, pp. 73–79, 2012.

[135] M. Kitamura, Y. Kuzumoto, W. Kang, S. Aomori, and Y. Arakawa, "High conductance bottom-contact pentacene thin-film transistors with gold-nickel adhesion layers," *Appl. Phys. Lett.*, vol. 97, no. 3, pp. 1–3, 2010.

[136] H. Minemawari *et al.*, "Inkjet printing of single-crystal films," *Nature*, vol. 475, no. 7356, pp. 364–367, 2011.

[137] Y. Yuan *et al.*, "Ultra-high mobility transparent organic thin film transistors grown by an off-centre spin-coating method," *Nat. Commun.*, vol. 5, no. 1, p. 3005, 2014.

[138] Y. Shimura *et al.*, "Specific contact resistances between amorphous oxide semiconductor In–Ga–Zn–O and metallic electrodes," *Thin Solid Films*, vol. 516, no. 17, pp. 5899–5902, 2008.

[139] J.-S. Park, J. K. Jeong, Y.-G. Mo, and H. D. Kim, "Improvements in the device characteristics of amorphous indium gallium zinc oxide thin-film transistors by Ar plasma treatment," *Appl. Phys. Lett.*, vol. 90, no. 26, pp. 1–3, 2007.

[140] R. Aga, C. Jordan, R. S. Aga, C. M. Bartsch, and E. M. Heckman, "Metal electrode work function modification using aerosol jet printing," *IEEE Electron Device Lett.*, vol. 35, no. 11, pp. 1124–1126, Nov. 2014.

[141] Y. Ueoka *et al.*, "Analysis of printed silver electrode on amorphous indium gallium zinc oxide," *Jpn. J. Appl. Phys.*, vol. 53, no. 4S, 2014, Art. no. 04EB03.

[142] H. Ning *et al.*, "Direct inkjet printing of silver source/drain electrodes on an amorphous InGaZnO layer for thin-film transistors," *Materials*, vol. 10, no. 1, p. 51, Jan. 2017.

[143] S. C. Lim *et al.*, "Contact resistance between metal and carbon nanotube interconnects: Effect of work function and wettability," *Appl. Phys. Lett.*, vol. 95, no. 26, pp. 1–3, 2009.

[144] P. Darmawan *et al.*, "Optimal structure for high-performance and low-contact-resistance organic field-effect transistors using contact-doped coplanar and pseudo-staggered device architectures," *Adv. Funct. Mater.*, vol. 22, no. 21, pp. 4577–4583, 2012.

[145] K. Fukuda, Y. Takeda, M. Mizukami, D. Kumaki, and S. Tokito, "Fully solution-processed flexible organic thin film transistor arrays with high mobility and exceptional uniformity," *Sci. Rep.*, vol. 4, no. 2, p. 3947, 2014.

[146] V. Shrotriya, G. Li, Y. Yao, C.-W. Chu, and Y. Yang, "Transition metal oxides as the buffer layer for polymer photovoltaic cells," *Appl. Phys. Lett.*, vol. 88, no. 7, p. 1–3, 2006.

[147] D. Kumaki, Y. Fujisaki, and S. Tokito, "Reduced contact resistance and highly stable operation in polymer thin-film transistor with aqueous MoO_x solution contact treatment," *Org. Electron.*, vol. 14, no. 2, pp. 475–478, 2013.

[148] Y. Ueoka *et al.*, "Effect of contact material on amorphous InGaZnO thin-film transistor characteristics," *Jpn. J. Appl. Phys.*, vol. 53, no. 3S1, 2014, Art. no. 03CC04.

[149] D. Kim, S. Jeong, H. Shin, Y. Xia, and J. Moon, "Heterogeneous interfacial properties of ink-jet-printed silver nanoparticulate electrode and organic semiconductor," *Adv. Mater.*, vol. 20, no. 16, pp. 3084–3089, 2008.

[150] A. Kumatani *et al.*, "Solution-processed, self-organized organic single crystal arrays with controlled crystal orientation," *Sci. Rep.*, vol. 2, no. 73, p. 393, 2012.

[151] C. Yang *et al.*, "Amorphous InGaZnO thin film transistor fabricated with printed silver salt ink source/drain electrodes," *Appl. Sci.*, vol. 7, no. 8, p. 844, Aug. 2017.

[152] J. Kim *et al.*, "All-solution-processed bottom-gate organic thin-film transistor with improved subthreshold behaviour using functionalized pentacene active layer," *J. Phys. D Appl. Phys.*, vol. 42, no. 11, 2009, Art. no. 115107.

[153] I. McCulloch *et al.*, "Liquid-crystalline semiconducting polymers with high charge-carrier mobility," *Nat. Mater.*, vol. 5, no. 4, pp. 328–333, Apr. 2006.

[154] J.-I. Han, G.-Y. Yang, and C.-H. Han, "A new self-aligned offset staggered polysilicon thin-film transistor," *IEEE Electron Device Lett.*, vol. 20, no. 8, pp. 381–383, Aug. 1999.
[155] T. Arai *et al.*, "Self-aligned fabrication process of electrode for organic thin-film transistors on flexible substrate using photosensitive self-assembled monolayers," *Jpn. J. Appl. Phys.*, vol. 46, no. 4B, pp. 2700–2703, 2007.
[156] W. S. Wong, E. M. Chow, R. Lujan, V. Geluz-Aguilar, and M. L. Chabinyc, "Fine-feature patterning of self-aligned polymeric thin-film transistors fabricated by digital lithography and electroplating," *Appl. Phys. Lett.*, vol. 89, no. 14, 2006, Art. no. 142118.
[157] H.-Y. Tseng and V. Subramanian, "All inkjet-printed, fully self-aligned transistors for low-cost circuit applications," *Org. Electron.*, vol. 12, no. 2, pp. 249–256, 2011.
[158] M. Ha *et al.*, "Aerosol-jet-printed, 1 volt H-bridge drive circuit on plastic with integrated electrochromic pixel," *ACS Appl. Mater. Interfaces*, vol. 5, no. 24, pp. 13198–13206, 2013.

RUIQIANG TAO received the B.E. degree in photoelectric technology from the South China University of Technology, Guangzhou, China, in 2014, where he is currently pursuing the Ph.D. degree in material physics and chemistry. His research interests currently include thin film transistors and solution-based film functionalization technologies.

HONGLONG NING received the B.S. degree in metal materials and fabrication in 1993, the M.S. degree in powder metallurgy in 1999, and the Ph.D. degree in electronic material and packaging in 2004. He is a Professor with the China South University of Technology. He worked in Korean Samsung from 2004 to 2013 as a Principle Researcher. He had published over 100 research papers and applied over 90 patents. His current research interests concern AMLCD, OLED, and E-Paper including flexible and print display materials and devices.

JIANQIU CHEN received the B.E. degree in photoelectric technology from the South China University of Technology, Guangzhou, China, in 2015, where he is currently pursuing the Ph.D. degree in material physics and chemistry. His research interests currently include oxide semiconductor materials, thin film transistors, and inkjet printing technology.

JIANHUA ZOU received the bachelor's degree in materials physics from North East University, China, in 2005 and the Ph.D. degree from the Physics Department, South China University of Technology in 2010, where he is currently an Associate Research Fellow with the School of Material Science and Engineering. His current research interests is device physics in organic electronics, including OLEDs and QLED. He has also published over 50 papers on high impact journals in the above areas.

ZHIQIANG FANG received the Ph.D. degree in pulp and paper engineering from the South China University of Technology (SCUT). He was a Visiting Scholar with the University of Maryland from 2012 to 2013, where he worked on transparent paper for flexible electronics under supervision of Prof. L. Hu. He joined in Prof. H. Ning's group with SCUT as a Post-Doctoral Fellow. His research interests include cellulose-based nanomaterials and biodegradable materials for functional paper and transparent paper for "green" flexible electronics.

CAIGUI YANG received the M.S. degree in material physics and chemistry from the South China University of Technology, Guangzhou, in 2018. His current research interests include thin film transistors based on printed silver electrodes.

YICONG ZHOU received the B.S. degree in electronic materials and components from the South China University of Technology, Guangzhou, China, in 2016, where he is currently pursuing the master's degree in material physics and chemistry. His research interests currently include inkjet-printed conductive materials, thin-film transistors, and post treatments.

JIANHUA ZHANG received the Ph.D. degree from Shanghai University in 1999. She is a Professor of Shanghai University. She was with the City University of Hong Kong as a Senior Visiting Researcher from 2001 to 2002. She was also a Post-Doctoral Fellow with the Department of Electrical Engineering and Computer Science, Heriot-Watt University, U.K. and Edinburgh Microelectronics Microsystems Research Center from 2002 to 2003. Her research interests currently include LEDs, TFTs, flexible devices, semiconductor processing and devices, and advanced packaging materials.

RIHUI YAO received the Ph.D. degree in optical engineering from Sun Yat-sen University in 2008. He is an Associate Professor with the China South University of Technology. His current research interests concern AMLCD, OLED, and E-Paper including flexible and print display materials and devices.

JUNBIAO PENG received the B.S. degree in physics from Jilin University in 1984 and the M.S. and Ph.D. degrees from the Changchun Institute of Physics, Chinese Academy of Sciences, in 1987 and 1993, respectively. He was a Post-Doctoral Fellow with the Korea Institute of Science and Technology and the National Institute of Materials and Chemical Research, Japan. In 2001, he joined the Institute of Polymer Optoelectronic Materials and Devices, South China University of Technology, as a Full Professor. His current research interests include design, characterization, and application of organic optoelectronic devices such as OLEDs, OPVs, and TFTs.